

Microstructural characterization of oxides formed on Cr-Al alloy coated accident tolerant fuel cladding after oxidation at 1200 °C in a steam environment

Dong Jun Park*, Yang Il Jung, Jung Hwan Park, Byoung Kwon Choi, Young Ho Lee, Hyun Gil Kim

Korea Atomic Energy Research Institute,

111 Daedeok-daero 989 beon-gil, Yuseong-gu, Daejeon, 34057, Republic of Korea

*Corresponding author: pdj@kaeri.re.kr

1. Introduction

Many studies have been devoted to developing an accident tolerant fuel (ATF) cladding, that can maintain its integrity for an extended period, in the event of an accident. One approach is to coat the existing Zr alloy cladding with oxidation-resistant high-temperature materials. In our previous research, we developed a Cr-Al alloy as a coating material, after consideration and screening of various materials as potential options [1].

In this study, we used a Cr-10 wt.% Al alloy to coat the Zr-based alloy to improve its temperature resistance during LOCA scenarios. Zr-based alloy samples coated with a Cr-Al layer were exposed to a temperature of 1200 °C in a steam environment. Uncoated Zr-based alloy was also exposed to the same test conditions to compare the efficacy of the coating layer. The microstructure and elemental distribution of the oxides formed on the surface of the Cr-Al alloy, the Cr-Al alloy matrix, and the interfacial region between the coated Cr-Al alloy and Zr-based alloy were analyzed in detail, using field emission transmission electron microscopy (FETEM). These results coincided with the high-resolution TEM (HRTEM) results. We found that depending on the distance from the surface, different oxides of Cr₂O₃ and Al₂O₃ were formed in the Cr-Al layer. It was expected that these protective and stable oxides near the surface of the Cr-Al layer would result in superior high-temperature oxidation resistance of the Cr-Al alloys.

2. Methods and Results

In this section some of the techniques used to form a coating layer on the Zr alloy cladding tube are described. The microstructure and elemental distribution of the oxides formed on the surface of Cr-Al alloys have been investigated and presented in detail.

2.1 Coating processes

A cathodic arc ion plating (AIP) technique was used to form the Cr-based Cr-Al alloy layer on the surface of Zr alloy samples. AIP is a high energy deposition process that employs a vacuum arc to generate ionized vapor from target materials [13]. Before coating, the surfaces of all Zr alloy specimens were ultrasonically cleaned in deionized water, acetone, and alcohol to remove any organic substances. Rotary and

turbomolecular pumps were used to evacuate the deposition chamber, and the base pressure was approximately less than 1×10^{-5} Torr. Prior to the deposition phase, the substrate was heated to 200 °C to remove humidity. The surface of the substrate was then sputtered to clean and remove contaminants and to facilitate better adhesion between the coating layer and the substrate. The arc current and the substrate bias voltage during the Cr-Al alloy layer deposition were 80 A and -200 V, respectively. High purity Ar gas (99.999%) was introduced into the deposition chamber to maintain the working pressure at 20 mTorr. The pressure of the Ar gas at the inlet was kept at 1×10^{-2} Torr during the deposition phase. The composition of the coated layer was determined to be Cr-based Cr-Al alloy containing 10 wt.% of Al. This optimum content of Al was determined through various test performed in our previous work [2].

2.2 Results

Cr-Al alloy-coated and uncoated Zr samples were exposed to the 1200 °C steam environment for 300 s. After oxidation, all the samples were cut, polished, and etched for OM analysis. Fig. 1 shows their cross-sectional metallographs obtained from OM. As shown in Fig. 1(b), ZrO₂, and oxygen-stabilized α -Zr(O) layers were formed due to oxygen diffusion during high-temperature steam exposure. In contrast, the Cr-Al alloy-coated (~20 μ m) Zr samples showed no significant oxidation at the outer surface and oxygen-stabilized α -Zr(O) layer in the Zr matrix, despite the same test conditions as the uncoated sample. In addition, the coated Cr-Al alloy layer remained tightly bonded to the matrix without exhibiting coating spallation and/or formation of defects such as cracks and pores. These results indicate that the Zr matrix can be adequately protected from 1200 °C steam exposure due to the coated Cr-Al alloy layer, which produces an improved high-temperature oxidation resistance.

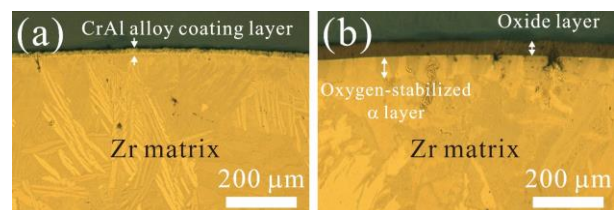


Fig. 1. OM images of a cross-sectioned (a) Cr-Al alloy-coated

and (b) uncoated Zr tube sample after the high- temperature oxidation test.

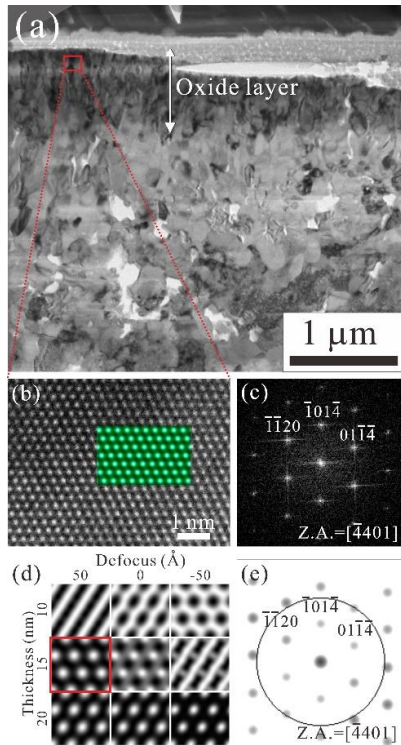


Fig. 2. Enlarged STEM image of the surface region of the Cr-Al alloy layer shown in Fig. 6 (a). (b) Experimental HRTEM image obtained at the dotted rectangle area in (a); the green rectangle represents the superposed simulated HRTEM image. (c) Fast Fourier transform (FFT) pattern obtained from (b). (d) A series of the simulated HRTEM images of the proposed Cr_2O_3 viewed along the $\langle 4-401 \rangle$ as a function of objective lens defocus, from -50 to 50 Å, and the specimen thickness, from 10 to 20 nm. (e) simulated DP with zone axis of $\langle 4-401 \rangle$.

For microstructural characterization of a more representative oxide layer formed on the Cr-Al alloy layer, the cross-sectional area near the surface region containing the entire oxide layer was characterized by STEM. Fig. 2(a) shows the bright-field STEM image obtained at the surface region. The darker area at the top (indicated by the white arrow) is the Cr oxide layer with a thickness of about $0.79 \mu\text{m}$. The Cr-Al alloy layer below the oxide layer shows equiaxed and smaller grains when compared to the Cr-Al layer near the interface between the coated layer and Zr matrix. HRTEM observations were performed to precisely determine the crystal structure of the Cr oxide layer near the surface (shown as the dotted red rectangle area in Fig. 2(a)), and the results are shown in Fig. 2(b). An FFT pattern of the region in Fig. 2(b) is shown in Fig. 2(c). Distances and angles between individual spots in the FFT pattern were quantified, and their indexing is presented above each spot. The analyzed structure of the oxide layer is in agreement with the atomic

arrangement of hexagonal close-packed (HCP) Cr_2O_3 along the $[4-401]$ zone axis. The NCEMSS software was used to obtain simulated lattice images and diffraction patterns of Cr_2O_3 . Fig. 2 (d) shows a series of simulated HRTEM images of the Cr_2O_3 along the zone axis of $[4-401]$ as a function of objective lens defocus, from -5 to -15 nm, and specimen thickness, from 10 to 30 nm. A simulated HRTEM image assuming an objective lens defocus of 50 and a specimen thickness of 15 nm was superimposed as the green rectangle onto the actual image in Fig. 2(b), and the simulation corresponded well with the actual result. The atomic d-spacing and angles of simulated DPs with a zone axis of $\langle 4(-)401 \rangle$ (Fig. 2(e)) were also in agreement with that of experimental DPs shown in Fig. 2(c).

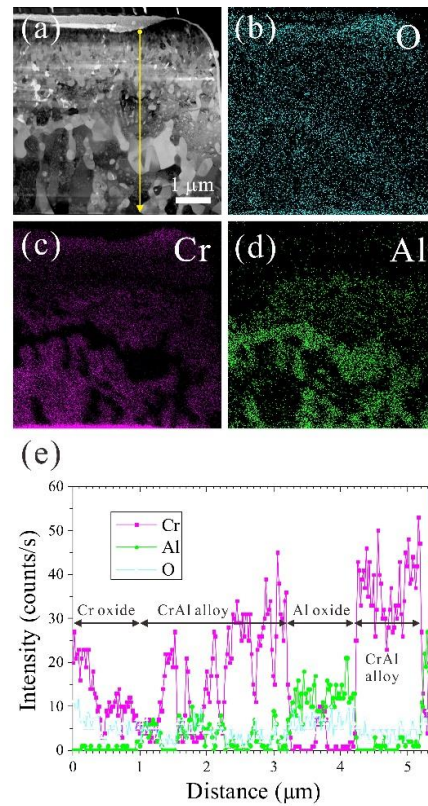


Fig. 3. (a) STEM image of an area close to the surface of the coated Cr-Al layer and EDS elemental mappings of (b) O (c) Cr, and (d) Al near the surface region. (e) EDS profiles recorded along the yellow line shown in Fig. 6(a).

In contrast to microstructure near the interfacial region, complex microstructures were observed near the outer surface region, as shown in Fig. 3(a). Figs. 3(b)-(d) show EDS elemental mapping along the cross-section near the surface region of the Cr-Al coating layer. Fig. 3(e) shows the EDS profiles from the surface to the coating layer, which is measured along the yellow line of Fig. 3(a). These results indicate that the coating layer near the outer surface consists of three phases: Cr oxide, Al oxide, and Cr-Al, as indicated in Fig. 3(e). The Cr oxide phase was formed on the outer surface of

the coated layer, and its thickness was about 1 μm . The Cr-Al alloy layer, including the Al oxide layer, was observed below the Cr oxide layer. Although the distribution of the Al oxide phase is uneven and somewhat irregular in some areas, it is generally distributed in the form of a long continuous strip lying perpendicular to the surface of the coatings.

3. Conclusions

Cr-Al alloy-coated Zr nuclear fuel cladding samples were oxidized in steam at 1200 °C to validate their high-temperature oxidation resistance and ascertain their potential as a candidate for ATF cladding. After high-temperature oxidation testing, the microstructures near the interface between the coating layer and Zr matrix and near the outer surface region were characterized using various analytical techniques.

Cr oxide phases such as Cr₂O₃, together with CrO₂, and CrO₃ were present near the outer oxide surface; the predominant phase was Cr₂O₃. The Cr-Al alloy layer below the Cr oxide showed a continuous long strip of an Al₂O₃ layer perpendicular to the surface. As a result, we concluded that this combination of Cr and Al oxide layers played a crucial role during exposure at high temperature and resulted in improved oxidation resistance compared to pure Cr.

REFERENCES

- [1] H. G. Kim, I. H. Kim, Y. I. Jung, D. J. Park, J. H. Park, B. K. Choi, Y. H. Lee, Out-of-pile performance of surface-modified Zr cladding for accident tolerant fuel in LWRs, *J. Nucl. Mater.* 510 (2018) 93-99.
- [2] NEA (2018), State-of-the-Art Report on Light Water Reactor Accident-Tolerant Fuels, Nuclear Science, OECD Publishing, Paris, <https://doi.org/10.1787/9789264308343-en>.